

# Conduction-band tight-binding description for Si applied to P donors

A. S. Martins,<sup>1</sup> Timothy B. Boykin,<sup>2</sup> Gerhard Klimeck,<sup>3</sup> and Belita Koiller<sup>4</sup>

<sup>1</sup>*Instituto de Física, Universidade Federal Fluminense, 24210-340, Niterói-RJ, Brazil*

<sup>2</sup>*Department of Electrical and Computer Engineering,  
The University of Alabama in Huntsville, AL 35899*

<sup>3</sup>*Network for Computational Nanotechnology, Electrical and Computer Engineering, Purdue University,  
IN 47907, and Jet Propulsion Laboratory, California Institute of Technology, CA 91109*

<sup>4</sup>*Instituto de Física, Universidade Federal do Rio de Janeiro, Cx.P. 68.528, 21945-970, RJ, Brazil*

(Dated: October 18, 2018)

A tight-binding parametrization for silicon, optimized to correctly reproduce effective masses as well as the reciprocal space positions of the conduction-band minima, is presented. The reliability of the proposed parametrization is assessed by performing systematic comparisons between the descriptions of donor impurities in Si using this parametrization and previously reported ones. The spectral decomposition of the donor wavefunction demonstrates the importance of incorporating full band effects for a reliable representation, and that an incomplete real space description results from a truncated reciprocal space expansion as proposed within the effective mass theory.

Advances in semiconductor device fabrication, particularly Si-based devices, have benefited from the progressive miniaturization and integration of their constituent parts, including detailed control of the doping process. The theoretical approach utilized for device modeling should be able to resolve charge-density variations on an atomic scale, and in this respect tight-binding (TB) models are particularly adequate, as they provide atomistic descriptions of structural and electronic properties of solids.<sup>1</sup> Since the pioneering work of Slater and Koster,<sup>2</sup> TB is conceived as an empirical method, where orbital energies and hoppings are parameters to be adjusted in order to reproduce relevant properties in the band structure of the solid. TB methods rely on the choice of a suitable parametrization of the Hamiltonian, which includes the choice of a basis set, range of hopping coupling, etc. For the group IV and III-V semiconductors one might expect that the minimal  $sp^3$  basis with first-neighbors coupling should suffice to describe the essential physics. However, this model is not able to reproduce the gaps of the indirect gap materials like Si and AlAs.<sup>3</sup> A simple scheme to correct this deficiency consists in introducing an excited  $s$ -like orbital,  $s^*$ , to improve the description of the conduction band (CB).<sup>4</sup> Another limitation of first-neighbor models based on  $s$  and  $p$  orbitals alone is that they predict an infinite value of the transverse effective mass at the  $X$  point. This anomaly may be overcome either by adding the five  $d$  orbitals in the first-neighbor basis set,<sup>5,6</sup> or by inclusion of second-neighbor (2nn) interactions in the  $sp^3s^*$  model.<sup>7</sup>

Comparison between the different TB parametrizations for Si available in the literature shows that the one that best reproduces the relevant bulk material properties is the one proposed by Klimeck *et al.*,<sup>8</sup> based on the first and second-neighbors  $sp^3s^*$  model. The reciprocal space position of the CB minima, however, is not well fitted. Silicon is an indirect gap material, with 6 CB minima along the equivalent  $\Delta$  lines, 85% of the way between  $\Gamma$  and  $X$ . In Ref. 8, a genetic algorithm (GA) fitting was adopted, and the target position for the min-

ima was considered as 75% between  $\Gamma$  and  $X$ . For some applications<sup>6,9</sup> it is known that a shift in the position of the CB minimum may lead to unsatisfactory results. We present here an improved parametrization, also obtained through the GA methodology,<sup>8</sup> reproducing the correct positions of the CB edges.

GA-based optimization employs stochastic methods which do not require constraints on continuity of solution space. In the case considered here, the TB parameters are varied in order to get an optimal set that reproduces given material properties, denoted as target values. Details on the method are discussed in Ref. 8: We refer to the parametrization published there as P075, and to the one proposed here as P085. Both parametrizations give the  $k$ -space positions of the six band minima at six equivalent points along  $\Delta$  lines, with the position of the minimum at  $\Delta_{min} = 0.75(2\pi/a_{Si})$  for P075 and  $\Delta_{min} = 0.85(2\pi/a_{Si})$  for P085, where  $a_{Si} = 5.431\text{\AA}$  is the conventional cubic lattice parameter for Si. Table I presents the TB parameters for Si for both parametrizations. The main difference between them consists in allowing non-zero 2nn hoppings  $V_{ss^*}(110)$  and  $V_{s^*s^*}(110)$  in the optimization set for P085. All 2nn hoppings are consistently smaller than the first-neighbors. The 2nn hopping parameters were determined to adjust the finer details of the target properties, and were not constrained to have values or signs expected from physical considerations.<sup>2</sup>

The input and the calculated properties are presented in Table II, where the first column shows the material properties to be represented by the TB model and the second column shows the corresponding experimental values.<sup>10</sup> These constitute the input targets in the GA code. The remaining columns give the calculated properties and the respective deviations from the experimental targets for P075 and P085, as well as for a recently proposed first-neighbor  $sp^3d^5s^*$  parametrization, which we denote by P1nn.<sup>6</sup> We note from Table II that the P075 and P085 parametrizations give consistently better agreement with the target values than the P1nn parametriza-

TABLE I: Parameters for the TB models (in eV).

Parameter	P075	P085
$E_s(000)$	-4.81341	-4.848054
$E_p(000)$	1.77563	1.787118
$E_{s^*}(000)$	6.61342	5.608014
$V_{ss}(\frac{1}{2}\frac{1}{2}\frac{1}{2})$	-8.33255	-8.259704
$V_{xx}(\frac{1}{2}\frac{1}{2}\frac{1}{2})$	1.69916	1.697556
$V_{xy}(\frac{1}{2}\frac{1}{2}\frac{1}{2})$	5.29091	5.351079
$V_{sp}(\frac{1}{2}\frac{1}{2}\frac{1}{2})$	5.86140	5.822197
$V_{s^*p}(\frac{1}{2}\frac{1}{2}\frac{1}{2})$	4.88308	4.864480
$\lambda_{SO}$	0.04503	0.014905
$V_{ss}(110)$	0.01591	0.029958
$V_{s^*s^*}(110)$	0.00000	0.191517
$V_{ss^*}(110)$	0.00000	0.007036
$V_{sx}(110)$	0.08002	0.161749
$V_{sx}(011)$	1.31699	0.885988
$V_{s^*x}(110)$	-0.00579	-0.095653
$V_{s^*x}(011)$	0.50103	0.966257
$V_{xx}(110)$	0.00762	0.037296
$V_{xx}(011)$	-0.10662	-0.132810
$V_{xy}(110)$	0.55067	0.619876
$V_{xy}(011)$	-2.27784	-2.496288

TABLE II: Optimization targets and optimized material properties for the P075, P085 and P1nn models. Except for  $\Delta_{min}$ , which is specific for different models, the target values correspond to experimental data given in Ref. 10.

Property	Target	P075	%dev	P085	%dev	P1nn	%dev
$\Delta_{min}$	0.750	0.758	1.067				
	0.850			0.8480	-0.235	0.813	-4.35
$E_c^\Gamma$	3.350	3.353	0.089	3.350	-0.013	3.399	1.44
$E_c^{\Delta_{min}}$	1.130	1.129	-0.050	1.130	-0.042	1.131	0.09
$m_{Xl}^*$	0.916	0.916	-0.030	0.916	0.050	0.891	-2.73
$m_{Xt}^*$	0.191	0.191	0.020	0.191	0.007	0.201	-5.23
$m_{lh}^*[001]$	-0.204	-0.198	3.082	-0.204	-0.060	-0.214	-4.90
$m_{lh}^*[011]$	-0.147	-0.146	0.525	-0.148	-0.568	-0.152	-3.40
$m_{lh}^*[111]$	-0.139	-0.139	0.395	-0.140	-0.610	-0.144	-3.60
$m_{hh}^*[001]$	-0.275	-0.285	-3.643	-0.277	-0.786	-0.276	-0.36
$m_{hh}^*[011]$	-0.579	-0.581	-0.338	-0.574	0.869	-0.581	-0.34
$m_{hh}^*[111]$	-0.738	-0.737	0.119	-0.727	1.466	-0.734	0.54
$m_{so}^*$	-0.234	-0.237	-1.487	-0.239	-2.162	-0.246	-5.13
$\Delta_{so}$	0.015	0.145	-0.067	0.015	0.030	0.016	4.90

tion. This statement cannot be generalized as a fundamental advantage of the second-neighbor  $sp^3s^*$  model over the nearest-neighbor  $sp^3d^5s^*$  model. The P1nn set<sup>6</sup> satisfies additional requirements beyond bulk behavior properties. On-going work indicates that the  $sp^3d^5s^*$  model can be fit to match the Si bulk properties just as well as the second-neighbor  $sp^3s^*$  model. The primary advantage of the nearest-neighbor  $sp^3d^5s^*$  model is

its straightforward incorporation of strain distortions.<sup>11</sup> In the donor description below, no strain distortions are considered, and the second-neighbor model P085 provides an unprecedented representation of the Si CB.

The reliability of TB  $sp^3s^*$  second-neighbors parametrizations has been recently verified by studies of shallow donors in GaAs<sup>12</sup> and in Si.<sup>13</sup> We perform the same kind of study here, and discuss the effect of the CB minimum position in different aspects of the donor problem. We write the Hamiltonian for the impurity problem as<sup>14</sup>  $H = \sum_{ij} \sum_{\mu\nu} h_{ij}^{\mu\nu} c_{i\mu}^\dagger c_{j\nu} + \sum_{i,\nu} U(R_i) c_{i\nu}^\dagger c_{i\nu}$

where  $i$  and  $j$  label the atomic sites,  $\mu$  and  $\nu$  denote the atomic orbitals and  $R_i$  is the distance between site  $i$  and the impurity site. The impurity potential is taken as a screened Coulomb potential,  $U(R_i) = -e^2/(\epsilon R_i)$  ( $\epsilon = 12.1$  for Si). At the impurity site it is assigned the value  $U(R_i = 0) = -U_0$ , a parameter describing central cell effects characteristic of the substitutional species, and taken here as an adjustable parameter. We do not include spin-orbit corrections in the present calculations.

The eigenstates of  $H$  are determined for a system where a single impurity is placed in a cubic supercell containing  $N = 8L^3$  atoms in the diamond structure, where  $L$  is the length of the supercell edge in units of  $a_{Si}$ . We adopt periodic boundary conditions, and large supercells<sup>12</sup> (up to  $10^6$  atoms) were treated within a variational scheme<sup>15,16</sup> where the ground state wavefunction and binding energy  $E_L$  are obtained by minimizing  $\langle \Psi | (H - \epsilon_{ref})^2 | \Psi \rangle$ . The reference energy  $\epsilon_{ref}$  is chosen within the gap, nearest to the CB edge.

The eigenfunctions of  $H$  in the basis of atomic-like orbitals are written as  $|\Psi_{TB}(\mathbf{r})\rangle = \sum_{i\nu} a_{i\nu} |\phi_\nu(\mathbf{r} - \mathbf{R}_i)\rangle$ , where the expansion coefficients  $a_{i\nu}$  give the probability amplitude of finding the electron in the orbital  $\nu$  at site  $\mathbf{R}_i$ . The overall charge distribution is conveniently described through the TB envelope function squared,<sup>17</sup>

$$|\Psi_{EF}(\mathbf{R}_i)|^2 = \sum_{\nu} |a_{i\nu}|^2. \quad (1)$$

In Fig. 1, a convergence study of the donor ground state binding energy as a function of the supercell size  $L$  is presented for P075 and P085. One can observe in Fig. 1(a) that for supercell sizes  $L > 25$  the calculated binding energies reproduce the experimental value ( $E_{exp} = 45.6$  meV) taking  $U_0 = 1.48$  and  $U_0 = 1.26$  eV for P075 and P085, respectively. We denote these values by  $U_P$ , as they are determined by tuning the on-site potential  $-U_0$  in order to give the converged value of  $E_b$  in agreement with experiment for P donors in Si. Fig. 1(b) presents a plot of  $\ln[(E_L - E_{exp})/E_{exp}]$  vs  $L$ . The linear behavior obtained here indicates *the same* exponential convergence of  $E_L$  to the experimental value for both parametrizations:  $E_L \sim E_{exp} + \tilde{E}e^{-L/\lambda}$ .

We determine the first excited state energy<sup>13</sup> by varying the value of  $\epsilon_{ref}$  in  $\langle \Psi | (H - \epsilon_{ref})^2 | \Psi \rangle$ . Keeping  $U_0 = 1.26$  eV, we obtain the binding energy of the first

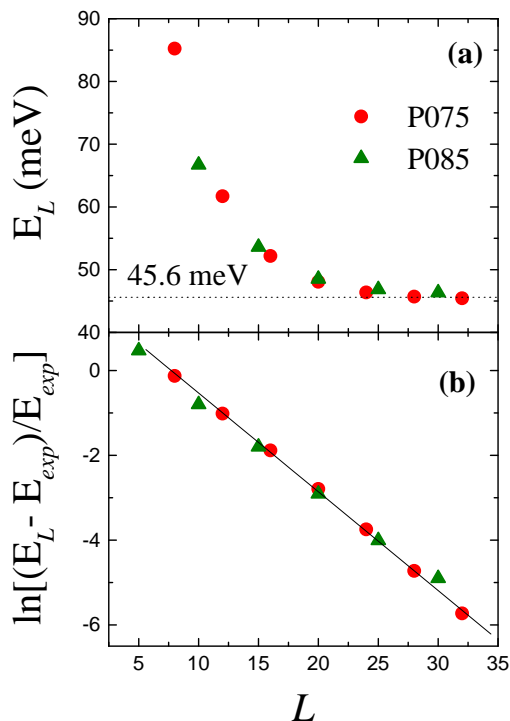


FIG. 1: (Color online) (a) Convergence of the donor ground state binding energy towards the experimental value (dotted line gives  $E_{exp} = 45.6$  meV) with the supercell size  $L$ , for  $U_0 = U_P$ , namely 1.48 eV and 1.26 eV for P075 and P085 respectively. (b) Same data plotted as  $\ln[(E_L - E_{exp})/E_{exp}]$  vs  $L$ . The linear behavior (the line is a best fit for all data points) indicates that the convergence of the binding energy with the supercell size  $L$  follows the same exponential law for both parametrizations.

excited state to be 30.2 meV, in good agreement with the P075 result, 32.4 meV.

The behavior of the binding energy with  $U_0$  is presented in Fig. 2(a), where the dotted lines indicate the value of  $U_P$  for each parametrization leading to  $E_b = E_{exp}$ . As noted in Ref. 13, in the weak perturbation limit the binding energies converge to the effective mass theory (EMT) prediction in its simplest formulation<sup>18</sup> (single-valley approximation),  $\sim 30$  meV. It is interesting that this behavior is the same for both parametrizations. As  $U_0$  increases, P085 tends to give higher binding energies than P075, resulting in a smaller value of  $U_P$ .

One can also characterize the donor ground state by its orbital averaged spectral weight<sup>17</sup> at  $\mathbf{k} = \Delta_{min}$ ,  $W(\Delta_{min}) = \frac{2}{N} \sum_{\mu=1}^6 \sum_{ij\nu} e^{i\mathbf{k}\mu \cdot (\mathbf{R}_i - \mathbf{R}_j)} a_{i\nu} a_{j\nu}$ , plotted in

Fig. 2(b) as a function of  $U_0$ . The EMT approach presumes that  $W(\Delta_{min}) \sim 1$ , allowing the donor state to be well described in a basis of Bloch states at the CB-edge  $\mathbf{k}$  points. However, one can notice in Fig. 2 (b) that this is not the case: Even for the smallest values of  $U_0$  the spectral weights at  $\Delta_{min}$  are well below saturation (one) for both parametrizations, implying that an incomplete description may result from EMT in this case.

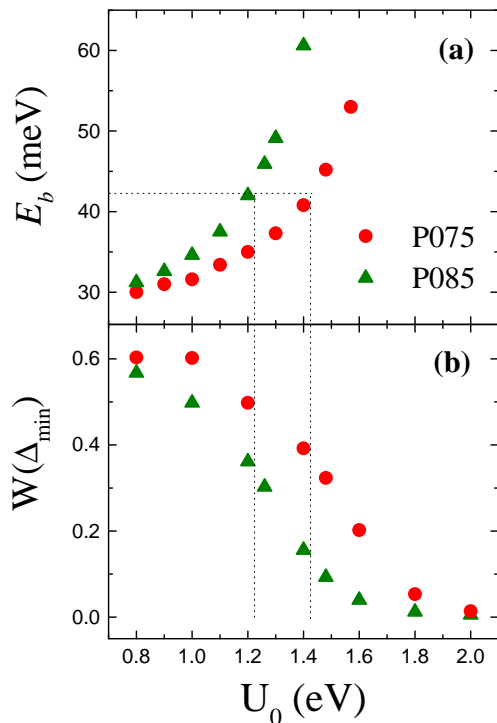


FIG. 2: (Color online) (a) Binding energy of the ground state as a function of the on-site perturbation strength  $U_0$ . The dotted lines indicate the value  $U_0 = U_P$  that reproduces the experimental Si:P  $A_1$  state binding energy. (b) Total spectral weight at the CB edges for the ground impurity state.

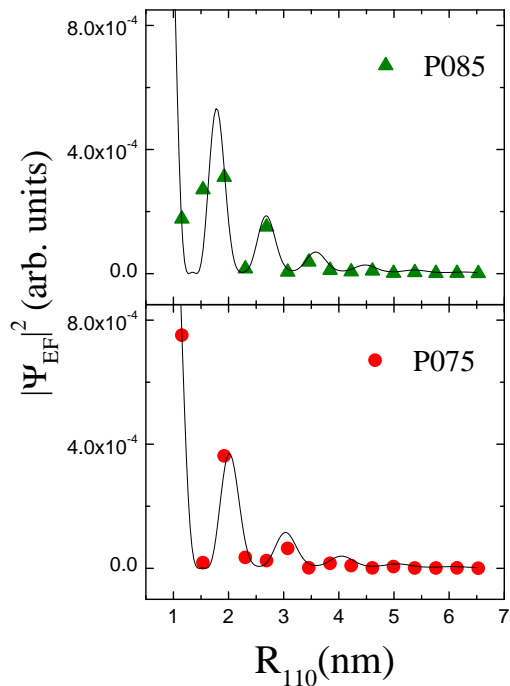


FIG. 3: (Color online) TB envelope function squared for the donor ground state along the  $[110]$  direction. The lines are the corresponding effective mass  $|\psi|^2$  results.

The spectral weight at  $U_P$  is 0.32 for P075 and 0.30 for P085. These relatively low spectral weights indicate that multiple  $\mathbf{k}$  points, other than those corresponding to the six CB-edges of Si, contribute to the donor wavefunction expansion within any reciprocal-space based approach.

Within single-valley EMT the ground state for donors in Si is six-fold degenerate.<sup>18</sup> Valley-orbit interactions<sup>19</sup> lead to a non-degenerate ground state wavefunction of  $A_1$  symmetry,

$$\psi(\mathbf{r}) = \frac{1}{\sqrt{6}} \sum_{\mu=1}^6 F_{\mu}(\mathbf{r}) u_{\mu}(\mathbf{r}) e^{i\mathbf{k}_{\mu} \cdot \mathbf{r}}, \quad (2)$$

where  $\phi_{\mu}(\mathbf{r}) = u_{\mu}(\mathbf{r}) e^{i\mathbf{k}_{\mu} \cdot \mathbf{r}}$  are the pertinent Bloch wavefunctions, and the envelope functions are given by  $F_z(\mathbf{r}) = (1/\sqrt{\pi a^2 b}) e^{-[(x^2+y^2)/a^2+z^2/b^2]^{1/2}}$  for  $\mu = z$  and equivalently for the other  $\mu$  values. The effective Bohr radii for Si are  $a = 2.51$  nm and  $b = 1.44$  nm.<sup>9</sup> Fig. 3 presents a comparison between the TB envelope function calculated from (1) along the [110] direction, for both P075 and P085 parametrizations (data points) with the corresponding EMT results obtained from (2) (solid lines), with  $a$  and  $b$  are given above, but with a different normalization to conciliate the TB and EMT wavefunctions on the same scale. The values of  $\mathbf{k}_{\mu}$  used in (1) are consistent with the respective reciprocal space location of the CB minima. Note that the oscillatory behavior due to interference among the plane-wave parts of the six  $\phi_{\mu}$  is well captured by the TB envelope function. The period of the oscillations is different for P075 and P085, as given by the corresponding wavevectors.

Good agreement between TB and EMT is restricted to distances from the impurity site larger than  $\sim 1$  nm. This means that at large distances the EMT expansion of the donor wavefunction in only six  $\mathbf{k}$  points, as given

in Eq.(2), is capable of reproducing its main features (except for normalization, of course). Closer to the impurity, particularly at the impurity site, the TB results become much larger than the EMT prediction.

The wavefunctions obtained from P085 and P075 agree reasonably well in the central cell region. One way to quantify this agreement is through the probability to find the donor electron inside of a sphere of radius  $R_c$ :  $Q(R_c) = \sum_{R \leq R_c} |a_{i\nu}(R)|^2$ . Taking for  $R_c$  the 2nn distance, the ratio of  $Q(R_c)$  obtained from the two parametrizations is  $Q_{P085}(R_c)/Q_{P075}(R_c) = 1.15$ .

In summary, we find good agreement between the results obtained within P085 and P075 for (i) the exponential convergence law for the ground state binding energy with supercell size, (ii) the binding energy of the first excited state, (iii) the spectral weight of the ground state wavefunction at  $\Delta_{min}$ , (iv) the probability that the donor electron is within the central cell up to the impurity's 2nn. Both parametrizations also capture the donor wavefunction oscillations predicted within EMT; the main difference regards the period of the oscillations. In applications where the quantitative aspects of the oscillatory behavior of the wavefunction is important, the P085 parametrization is thus capable of providing a better description. The importance to represent the P impurity wavefunction in a full band, atomistic representation is demonstrated through its spectral decomposition, and by direct comparison between the TB results and EMT.

**Acknowledgments** We thank F.J. Ribeiro for fruitful discussions. BK thanks the hospitality of CMTC at the University of Maryland. This work was partially supported in Brazil by FAPERJ, CAPES, FUJB, Instituto do Milênio de Nanociências/MCT, and at the Jet Propulsion Laboratory, Caltech by NASA. Funding for GK was provided by JPL, NASA-ESTO, ARDA, ONR, and NSF.

- 
- <sup>1</sup> Aldo Di Carlo, *Semicond. Sci. Technol.* **18**, R1 (2003), and reference therein.
- <sup>2</sup> J. C. Slater and G. F. Koster, *Phys. Rev.* **94**, 1498 (1954).
- <sup>3</sup> D. J. Chadi and M. L. Cohen, *Phys. Status Solid B* **68**, 405 (1975).
- <sup>4</sup> P. Vogl, H. P. Hjalmarson, and J. D. Dow, *J. Phys. Chem. Solids* **44**, 365 (1983).
- <sup>5</sup> J.-M. Jancu, R. Sholz, F. Beltram, and F. Bassani, *Phys. Rev. B* **57**, 6493 (1998).
- <sup>6</sup> T. B. Boykin, G. Klimeck, and F. Oyafuso, *Phys. Rev. B* **69**, 115201 (2004).
- <sup>7</sup> T. B. Boykin, *Phys. Rev. B* **56**, 9613 (1997).
- <sup>8</sup> G. Klimeck, R. C. Bowen, T. B. Boykin, C. S.-Lazaro, T. A. Cwik, and A. Stoica, *Superlattices and Microstructures* **27**, 77 (2000).
- <sup>9</sup> B. Koiller, X. Hu, and S. Das Sarma, *Phys. Rev. Lett.* **88**, 27903 (2002).
- <sup>10</sup> O. Madelung, *Semiconductor-Basic Data* (Springer-Berlin, 1996).
- <sup>11</sup> T. B. Boykin, G. Klimeck, R. C. Bowen, and F. Oyafuso, *Phys. Rev. B* **66**, 125207 (2002).
- <sup>12</sup> A. S. Martins, J. G. Menchero, R. B. Capaz, and B. Koiller, *Phys. Rev. B* **65**, 245205 (2002).
- <sup>13</sup> A. S. Martins, R. B. Capaz, and B. Koiller, *Phys. Rev. B* **69**, 085320 (2004).
- <sup>14</sup> J. G. Menchero, R. B. Capaz, B. Koiller, and H. Chacham, *Phys. Rev. B* **59**, 2722 (1999).
- <sup>15</sup> R. B. Capaz, G. C. de Araujo, B. Koiller, and J. P. von der Weid, *J. Appl. Phys.* **74**, 5531 (1993).
- <sup>16</sup> L. W. Wang and A. Zunger, *J. Chem. Phys.* **100**, 2394 (1994).
- <sup>17</sup> T. G. Dargam, R. B. Capaz, and B. Koiller, *Phys. Rev. B* **56**, 9625 (1997).
- <sup>18</sup> W. Kohn, *Solid State Physics Series*, vol. 5 (Academic Press, 1957).
- <sup>19</sup> A. Baldereschi, *Phys. Rev. B* **1**, 4673 (1970).